TECHNO-ECONOMIC ANALYSIS OF HALF CELL MODULES - THE IMPACT OF HALF CELLS ON MODULE POWER AND COSTS

Max Mittag, Andrea Pfreundt, Jibran Shahid, Nico Wöhrle, Dirk Holger Neuhaus
Fraunhofer Institute for Solar Energy Systems ISE, Heidenhofstr. 2, 79110 Freiburg, Germany
max.mittag@ise.fraunhofer.de

ABSTRACT: Modules using halved cells are a promising development to improve module power and reduce module costs. We perform an analysis of power gains and losses within half-cell modules using the cell-to-module (CTM) methodology and find an increase in internal reflection (backsheet gains) as well as a reduction in electrical losses to be the main influence for a power gain of half-cell modules. The CTM power ratio increases by 2-4% for half-cell modules. We perform a Cost of Ownership (CoO) calculation and find the absolute costs (€) of half-cell modules to be 0.6-1.2% higher than for a comparable full cell reference. The specific costs (€/Wp) of half-cell modules are 0.8-1.0% lower due to the CTM power gains.
Keywords: CTM, half-cell, module efficiency, module design, cost calculation, temperature, performance, optimization, analysis

1. INTRODUCTION

The separation of solar cells and the subsequent interconnection of halved cells has been presented earlier and many commercial applications are known [1]. It is advertised and reported that the concept features advantages regarding module costs, power, efficiency, reliability and performance within power plants compared to full size cells [2, 3]. The share of half-cell modules therefore is expected to increase significantly within the next years [4].

We perform a cell-to-module (CTM) analysis and investigate influencing factors to evaluate possible power and efficiency gains of half-cell modules compared to full cell references. We use a known and well established methodology to analyze the CTM gains and losses [5–7]. The technical analysis is performed using detailed and validated models for geometrical, optical, electrical and thermal effects influencing the module power [8–12]. The CTM analysis uses over 100 input values and calculates 15 different major influence factors that are linked to physical effects (i.e. absorption) or to major module components (i.e. the cell interconnector ribbon). Calculations are performed using the software "SmartCalc.CTM" (version 1.2.1) developed by Fraunhofer ISE.

We analyze the impact of different module design options (cell dimensions, cell spacing, total module size and active area share) and their relevance for the half-cell module. The technical analysis is combined with a cost model [13, 14]. We include material, process, capital and other relevant cost factors into this analysis and evaluate the impact of half-cells on specific costs (€/Wp).

The combination of CTM analysis and cost modelling allows for a techno-economic analysis and subsequent optimization, which is highly relevant for module producers.

2. HALF-CELL MODULE DESIGN

When switching from full cells to half-cells several options are available regarding the module design. When maintaining the module area and the cell spacing (compared to a full cell reference) it is necessary to reduce the active area (Figure 1, b). Keeping the active area share constant but increasing the number of solar cells within the module will require a change in cell spacing (c). When maintaining spacings and active area share, a change module size is the consequence (d). Beside cell and string spacing also distances from the solar cell to the module edge (frames) may have to be altered.

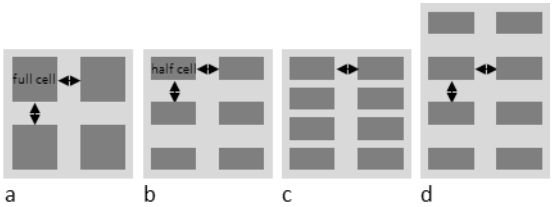

Figure 1: Implications of the introduction of half-cells regarding active area, cell spacing and module size.

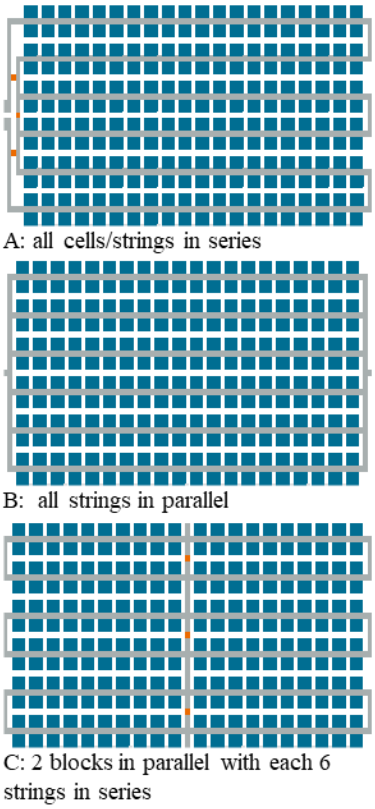

Figure 2: Different module topologies for half cell modules, blue = solar cell, grey = interconnector, orange = bypass diode.

Additional spacings may be introduced in half cell modules to consider changes in module topology and for placement of bypass diodes and junction boxes. Different options are available and some examples are shown in Figure 2 to illustrate the impact.

While topology A and B do not introduce additional elements into the module design, the final module will have a change in electrical output regarding the current-voltage characteristics compared to a conventional full cell module design. Design C has similar IV characteristics compared to a full cell module but features additional interconnector ribbons and spacings. Also note that the implementation of bypass diodes is different for each topology, which requires additional changes in junction box design and positioning.

A change in topology may result in differences between the designs in outdoor operation especially considering partial shading, inhomogeneous irradiance due to mounting situations (view factor consideration on tilted modules for "portrait" or "landscape" mounting of modules). To assess the effects of such changes in photovoltaic systems a holistic approach is required [15].

Beside the changes in IV characteristics and the introduction of additional elements or changes in the Bill of Materials (BOM) a third important impact of half cells are changes in module manufacturing and related processes.

3. CELL-TO-MODULE ANALYSIS

3.1. Modelling Setup Description

For the CTM analyses we assume a full square PERC cell based on the M4 wafer format (161.75 mm base length). The cells have six busbars, 130 fingers, and conventional front side optics with random pyramid texture and anti-reflection nitride (simulated with SunSolve [16]). The 180 µm thick p-type Si base has 2 Ωcm resistivity and a BO-regenerated minority carrier lifetime of τ_n = 2400 µs [16] and a boron emitter diffusion (j_{0e} = 50 fA/cm²). The rear side is capped with a conventional AlO_x/SiN_x passivation stack and contacted with full area aluminum through line openings (implying an Al-BSF).

Cut solar cells may not feature half the power of the initial full cell due to additional losses from cell separation such as edge recombination [17–19]. For our calculations we chose two different routes to consider those possible losses from the cell separation process.

Firstly, we assume a solar cell that features significant edge recombination losses embodied by the parameters $j_{02,edge}$ = 19 nA/cm [18] and $S_{eff,edge} = 5 \cdot 10^6$ cm/s in a Quokka3 [20] simulation. Results are shown in Table I. The cells suffering from edge losses yield decreased FF and V_{OC} [19] and thus exhibit a power output lower than half of the full cell. CTM-factors and module power will be impacted by that change which complicates discussion of results.

For CTM analysis, we therefore assume a second half cell, that is the result of a perfect process (e.g. by an edge passivation step) yielding exactly the power per area of the full cell. This cell is used as an upper boundary while the cell with edge recombination represents the lower boundary of our confidence interval to evaluate possible advantages of the half cell module designs.

Table I: Cell parameters for CTM-analysis

	full cell	half cell	
		edge losses	perfect
length [mm]	161.75	80.88	80.875
width [mm]	161.75	161.75	161.75
efficiency [%]	22.34	22.04	22.34
I_{SC} [A]	10.46	5.23	5.23
V_{OC} [V]	0.683	0.681	0.683
P_{MPP} [W_p]	5.84	2.88	2.92
I_{MPP} [A]	10.00	4.97	5.00
V_{MPP} [V]	0.585	0.580	0.585
fill factor [%]	81.78%	80.94%	81.78%
metalized area [mm]	888	444	444

We will first perform CTM analyses using the cells with edge losses to evaluate, if the losses in cell splitting directly translate to module power losses. We will then perform CTM analyses with perfect half cells to compare the different module design options.

It is known that a change in cell spacing will affect the gains from internal reflection ("backsheet gain") [10, 21]. This gain is an additional irradiance on the solar cell that leads to an increase in cell current which then increases electrical losses in the cell interconnectors. Different loss channels within PV modules are linked and optical performance and electrical losses cannot be separated in a calculation. We use a model that takes these dependencies into account and uses the cell-to-module ratio as a key parameter to describe the impact of the integration of solar cells into modules [2].

We analyze four different concepts as shown in Figure 1 and described in Table II. A module topology as pictured in Figure 2 (a) is assumed. For reasons of simplicity additional spacing elements i.e. resulting from a change in topology (Figure 2) are not considered here.

Table II: Module design specifications

setup	a	b	c	d
cells [pcs]	6x10	6x19	6x20	
length [mm]	1713.5			1753.5
width [mm]	1030.5			
cell spacing [mm]	4		1.89	4
string spacing [mm]	4			
frame top/bottom [mm]	30	52.4	30	
frame left/right [mm]	20			
module area [m²]	1.766			1.807
cell area [m²]	1.57	1.49	1.57	
active area share [%]	88.9	84.5	88.9	86.9

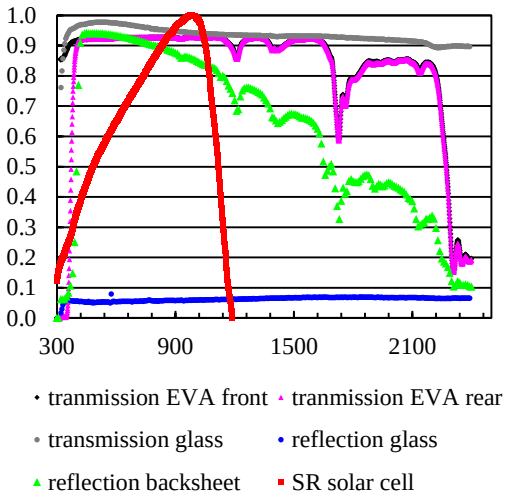

Figure 3: Optical parameters of the materials used in the CTM-analyses

Commercial module materials such as encapsulants, backsheets and ribbons are used for calculation. The low-iron front glass has a thickness of 3.2 mm and is equipped with an anti-reflection coating. Optical parameters of the materials have been characterized at Fraunhofer ISE and are shown in Figure 3. The front encapsulant film (EVA, 0.45 mm thickness) is assumed to have a low UV cut-off while the rear encapsulant has a cut-off at higher wavelengths. Note that the characterization has been performed beyond the spectral response (SR) of the solar cell to improve thermal modelling.

We extend the simulation to operation conditions beyond laboratory testing (STC) and perform a variation of irradiance from 100 to 1200 W/m². Irradiance is direct normal with an AM1.5g spectrum and from the module front only. We did not use irradiance from the module rear side for this calculation (albedo = 0).

We perform this variation twice. In the first simulation, the cell and cell temperature is set to 25 °C (STC). For the second calculations we set ambient temperature and ground temperature to 25 °C but calculate the cell temperatures at each irradiance level. To calculate the cell temperature we assume a 45° tilted mounting and a wind speed of 1 m/s. We calculate the module power at different irradiances (cell temperature = 25 °C) using the input values for each solar cell as described in Table I (full cell, perfectly split cell). We use this STC input and calculate the cell IV curves for each of the irradiances using a 1-diode-model. Sophisticated effects within the solar cell such as an increase in edge recombination at low irradiances for half-cells or extended low light behavior have not been considered yet.

3.2. Results of CTM Analysis (STC)

We calculate the module power and the respective CTM ratio for each setup using the half cell with edge losses and the perfectly split cells as an input. The detailed CTM analysis shows significant differences between the module concepts. For setups c and d (which use the same active area as the full cell module as an input) the module power loss from edge losses can be seen in the initial cell power: 4.6 Wp are lost compared to the full cell.

Table III: Module power, efficiency and CTM for different setups, half cells with edge recombination.

module setup	a	b	c	d
cell power [W_p]	350.6	328.7	346.0	
module power [W_p]	341.6	332.3	346.4	349.2
CTM_{power}	0.97	1.01	1.00	1.01
cell efficiency [%]	22.33	22.04		
module efficiency [%]	19.35	18.82	19.61	19.32
$CTM_{efficiency}$	0.87	0.85	0.89	0.88

Table IV: Module power, efficiency and CTM for different setups, half cells without edge recombination.

module setup	a	b	c	d
cell power [W_p]	350.6	333.0	350.6	
module power [W_p]	341.6	336.9	351.1	354.0
CTM_{power}	0.97	1.01	1.00	1.01
cell efficiency [%]	22.33			
module efficiency [%]	19.35	19.08	19.88	19.59
$CTM_{efficiency}$	0.87	0.85	0.89	0.88

Both sets of calculations result in very similar CTM_{power} ratios ($\Delta < 0.07\%_{rel.}$). Losses in cell splitting directly translate to module power losses with our setup and under Standard Testing Conditions (STC).

We are going to use that in the following discussion of the impacts of different module designs. We will base the discussion on simulations using the perfectly split half cells as an input. By doing so, we achieve a better compatibility since no cell effects but only module effects have to be considered when evaluating different module designs. Detailed analyses of the modules are shown in Figure 4 and Figure 5.

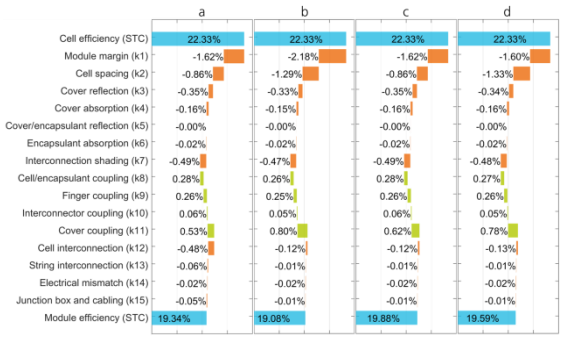

Figure 4: CTM analysis (efficiency) for different module designs, half cells are perfectly split.

Figure 5: CTM analysis (power), half cells are perfectly split.

As shown Table IV, option b (reducing the active area within the module to maintain module dimensions and spacings) leads to a lower module power compared to the full cell module and therefore a lower efficiency. On the other hand, design b and all other half-cell modules have a higher CTM_{power} ratio than the full cell module and a ratio > 1, which is favorable for non-vertically integrated module manufacturers since the CTM gains increase the profit share of such module manufacturers.

The changes in cell spacing and frames lead to significant changes in the geometrical loss factors k_1 and k_2 (Figure 4). Half cell modules typically feature more cell spacing area due to the increased number of cell spacings. Related backsheet gains are dependent on the cell distance as can be seen when comparing the module setups. While c has more spacings than b, spacing is reduced from 4 to 1.89 mm finally resulting in lower gains.

The changes in module design have an impact on the interconnection losses due to the altered length of the cell connector ribbons (reduction in series resistance). Additionally, the current of split cells is reduced compared to full cells. As expected, electrical losses (k_{12}, k_{13} and k_{15}) are significantly lower for all half cell modules.

We see that basic design decisions have a significant impact on module power and efficiency. Setup d has a 3.6% higher power output than the full cell module while setups b and c have -1.4% and +2.8%, respectively. An increase in module size as predicted by ITRPV [4] may therefore not only be driven by an increase of solar cells per module (full cell equivalents), but also by an optimized half cell module design (d).

3.3. Results of CTM Analysis (non-STC)

We calculate the module power at different irradiances (cell temperature = 25°C) and find the module power to increase with irradiance. We calculate a normalized module efficiency for each setup and irradiance to compare the different module designs (Figure 6) and find that an increase in irradiance does not linearly translate into a power gain. The full cell module performs relatively better than the half cell module at low irradiances.

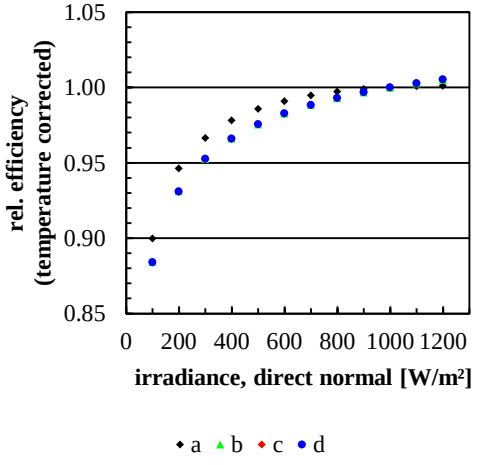

Figure 6: Normalized module efficiency of different module setups at different irradiances (cell temperature = 25 °C).

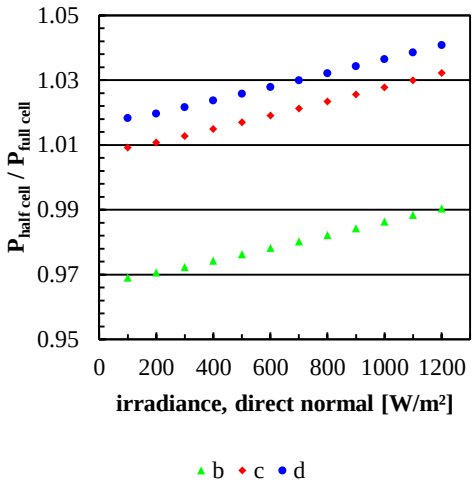

Figure 7: Ratio of the module power of different module setups to the module power of the full cell design at different irradiances (cell temperature = 25 °C).

We compare the output of each half cell setup with the full cell module and find the ratio to be clearly dependent on the irradiance (Figure 7). We see the advantage of the half cell designs with a higher module STC power (c, d) to be increasing with irradiance; the disadvantage of the half cell module with a lower nameplate power (b) to be decreasing with irradiance.

Losses in the full cell module are comparatively high due to the higher currents and the higher series resistance of the interconnection. This leads to an increase in resistive CTM power losses (see k_{12}, k_{13}, k_{15}). This increase limits power production of the full cell module at higher irradiances and leads to an advantage of the half cell designs. Our findings confirm previous work showing an increasing advantage of half cells at higher irradiance [2].

We now change the simulation setup and calculate the cell temperature and its impact on module power for every setup based on the respective module properties and operation conditions using an integrated thermal model [12]. Again we calculate a normalized module efficiency (Figure 8).

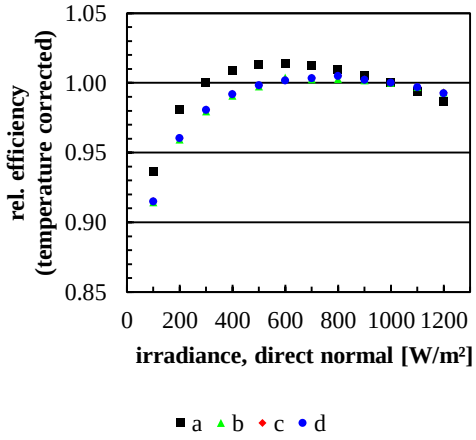

Figure 8: Normalized module power of different module setups at different irradiances (ambient temperature = 25 °C, wind speed = 1 m/s, 45° module inclination); cell temperature calculated, results normalized to 25 °C

We observe a change in the behavior due to the additional consideration of cell temperature. We find the operation at lower irradiances to be comparatively better for all module designs (Figure 8). Again, the full cell module has a relative advantage at lower irradiances when considering irradiance and STC nameplate rating.

We compare the output of each half cell setup with the full cell module and still find advantageous properties of the half cell modules (Figure 9). Advantages are increasing with irradiance. Adding the consideration of cell temperature leads to more beneficial behavior than only considering irradiance (Figure 7) and a nonlinear increase with irradiance.

Module characterization is typically performed at Standard Testing Conditions (STC: 1000 W/m², 25 °C). Therefore power gains of half-cell modules might not be considered correctly when it comes to outdoor operation and only STC-values are used as an input.

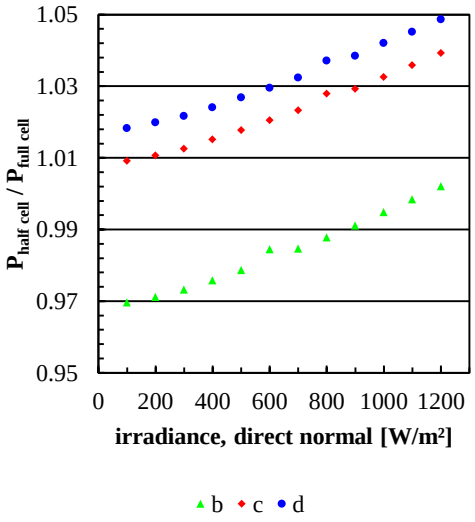

Figure 9: Ratio of the module power of different module setups to the module power of the full cell design at different irradiances (cell temperature = 25 °C).

To further evaluate the influence of the temperature on the behavior of different module concepts we analyze the cell temperature and influencing factors of the different designs.

Light incident on the PV module is either reflected, absorbed or transmitted. Light that is reflected or transmitted does not contribute to heating, light that is absorbed is producing heat – or in the case of the solar cell also electricity.

Solar cells typically do absorb more light than inactive module materials (white backsheets etc.). Since their efficiency is limited, most of the irradiant energy is converted to heat. Thus, modules with a larger active area share tend to be warmer than modules with the same size but a lower cell density.

Electrical power generated by the solar cells is contributing to the heating of the module via resistive losses in the interconnection [22]. This heating contributes to the cell temperature in a much lower extent than imperfect energy conversion in the solar cell [23]. Therefore, a reduction in electrical losses will lower the cell temperature.

Also optical CTM gains and losses influence the module temperature. Internal reflections are relevant for heat generation. Light reflected onto the solar cell will increase the module power. At the same time only a fraction of this light is converted to electricity while the majority of light generates excess heat [23]. This leads to modules that can have an elevated temperature due to improved light management.

We calculate the cell temperature and find no conditions, where the analyzed half cell modules are significantly warmer than the full cell module (Table V).

Table V: Cell temperature [°C] of each module setup at different irradiances and difference of each module setup compared to the full cell module design [K].

W/m²	a	b	c	d	b-a	c-a	d-a
100	26.0	26.0	26.1	26.0	0.0	0.1	0.0
200	29.8	29.7	29.8	29.8	-0.1	0.0	0.0
300	33.5	33.3	33.6	33.5	-0.2	0.1	0.0
400	37.2	36.9	37.3	37.2	-0.3	0.1	0.0
500	40.9	40.5	40.9	40.9	-0.4	0.0	0.0
600	44.5	44.0	44.6	44.5	-0.5	0.1	0.0
700	48.1	47.6	48.2	48.1	-0.5	0.1	0.0
800	51.7	51.1	51.8	51.7	-0.6	0.1	0.0
900	55.3	54.6	55.4	55.3	-0.7	0.1	0.0
1000	58.9	58.1	58.9	58.8	-0.8	0.0	-0.1
1100	62.5	61.6	62.5	62.4	-0.9	0.0	-0.1
1200	66.1	65.1	66.1	65.9	-1.0	0.0	-0.2

Temperature differences to the full cell reference are below 1 K in our scenarios. In setup b, the active cell area is reduced. Since solar cells are highly absorbing and have a limited conversion efficiency, they are the most dominant heat source within a conventional module. Setup b is therefore only cooler due to the lower cell area and the larger white backsheet area which is absorbing light at a lower rate. Setups a and c share the same module area and the same cell area. The temperature difference between both designs is therefore caused by effects related to different CTM ratios only.

Results indicate that for glass-backsheet modules no relevant advantage of half cells can be assumed in terms of operating temperature. For glass-glass designs additional advantages can be found [12].

The module temperature is the result of several impact factors such as power output, ambient conditions or module design that influence each other. While the operating temperature itself is not generally different for half cells, its impact has to be considered when analyzing the module performance as can be seen when comparing Figure 6 and Figure 8 or Figure 7 and Figure 9.

4. TECHNO-ECONOMIC ANALYSIS

4.1. Modelling Setup Description

We model the cost of ownership for the module designs using the “SCost” model (version 4.1) developed by Fraunhofer ISE [13, 14]. The cost model is based on the SEMI E10 and E35 standards and considers the costs of materials, processes, capital, labor, yield losses, maintenance, unplanned downtime and other relevant inputs. Important input parameters for materials and equipment are shown in Table VI and Table VII. Prices are based on market research. Manufacturing equipment data is extracted from technical datasheets and based on a

market research. Please note that costs and prices may be different i.e. for different regions, order quantities, quality levels or customer-vendor-relationships. Please consider this data as an orientation.

Table VI: Material price assumptions

glass 3 mm ARC	€/m²	5.50
EVA	€/m²	1.00
backsheet PET	€/m²	1.50
cell ribbon	€/kg	13.00
string ribbon	€/kg	11.50
junction box	€/pcs	4.30
frame	€/pcs	9.00
frame tape	€/m	0.15
label	€/pcs	0.07
solar cells, mono	€/Wp	0.12

Table VII: Equipment price assumptions

glass loader / washer	€/pcs	200,000 €
foil handling	€/pcs	150,000 €
stringer 2100 cells/h	€/pcs	350,000 €
string layup	€/pcs	200,000 €
cell splitting	€/pcs	300,000 €
string connection	€/pcs	300,000 €
laminator	€/pcs	600,000 €
edge trimming	€/pcs	200,000 €
junction box mounting	€/pcs	200,000 €
framing	€/pcs	200,000 €
flasher	€/pcs	300,000 €
module sorter	€/pcs	300,000 €

We assume a three shift production working 8760 h/a with a capacity of 239 to 252 MWp/a (depending on the module setup). Initial investments in buildings are assumed to be 3 Mio €. No additional costs for R&D, sales, general administration or other overhead costs are included.

4.2. Results of the techno-economic analysis

The analysis shows for all designs that 90% of the costs are related to materials (Figure 10). Solar cell costs dominate the material cost share with approximately 55% of the total material costs which confirms calculations by ITRPV [4]. Equipment is 2.1-2.4%, infrastructure 0.4-0.5%, labor 1.9-2.1% and utilities 4.9-5.0% in our calculation. The large share of solar cell costs still acts as a strong argument for CTM optimization to maximize power output related the non-cell-materials. An increase in CTM_{power} ratio without increasing module costs will result in an advantage regarding specific costs.

We find the total cost per module to be the lowest for setup b due to the reduced active cell area (Table VIII). All other half-cell modules have higher absolute costs (€) compared to the reference due to the additional cell splitting process step. The specific costs (€ct/Wp) are lower for setup c and d compared to the full cell reference due to the CTM power gains.

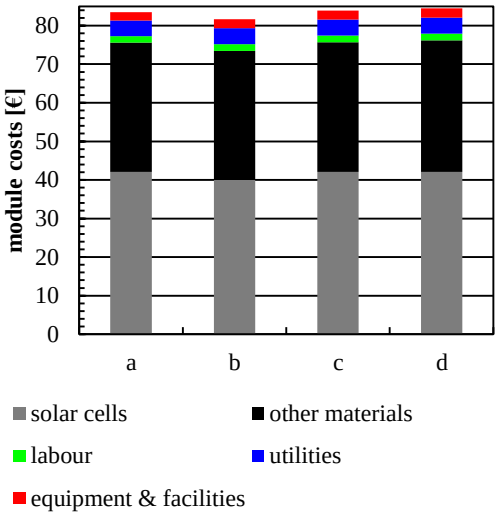

Figure 10: Cost structure of the different module productions by type of costs

Table VIII: Module costs

	a	b	c	d
€/module	84.03	82.28	84.52	85.05
rel. to full cell [%]	100.0	97.9	100.6	101.2
€ct./Wp	24.27	24.42	24.07	24.02
rel. to full cell [%]	100.0	100.6	99.2	99.0

The additional material costs of design d (increase in module size) compared to design c are compensated by the CTM_{power} gains. Specific costs are lowest for design d which combines a large active area share (Table II) with the highest CTM_{power} ratio (Table III). The increase in module efficiency of design c by reducing the cell spacing leads to a reduction in CTM_{power} gains, which results in higher specific costs.

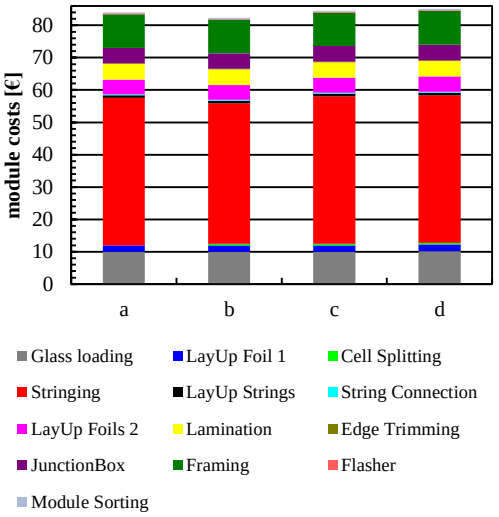

Figure 11: Cost of Ownership analysis (€/module) for the different module setups and process steps

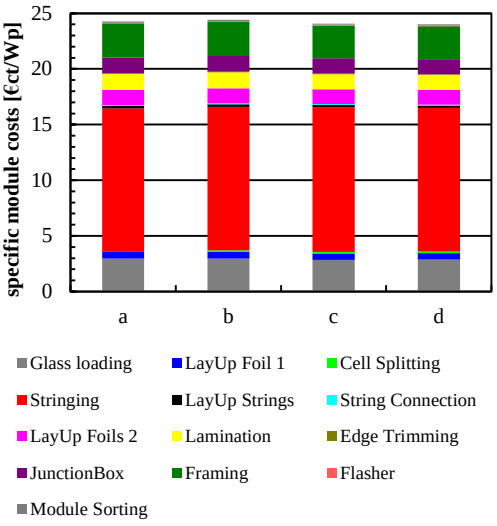

Figure 12: Cost of Ownership analysis (€ct/Wp) for the different module setups and process steps

5. SUMMARY & CONCLUSION

We perform a cell-to-module (CTM) analysis of different module concepts and identify critical design parameters. Switching from full cells to half-cells will impact the number of cells per module, the module size or the internal spacing and will subsequently influence gains and losses within the PV module.

We analyze the CTM gains and losses and find an increase in module size to be favorable in terms of power output. All examined half cell module designs have a higher CTM_{power} ratio than the full cell module. Power gains of up +3.6% and an efficiency gain of $0.5\%_{abs}$ are calculated for half cell modules.

We extend the CTM-analyses to realistic conditions and perform a variation in irradiance. We find the advantages of half-cell modules to be depending on the irradiance.

We conclude from the different behavior of the compared concepts that a laboratory characterization at Standard Testing Conditions (STC) is insufficient to evaluate new module designs for outdoor operation and performance. We did not quantify the impact on yield within this study and will present such analysis in future work.

We perform a Cost of Ownership (CoO) calculation and identify the material costs to be the dominant cost factor in module production accounting for 90% of the total CoO. Solar cells are the most important single component accounting for half of the total module costs.

We find half-cell modules to have higher absolute costs (€) compared to full cell equivalents due to the necessary additional process step (cell splitting).

A possible advantage of half cell designs regarding specific costs (€/Wp) depends on the module design. If the active cell area is maintained when switching from full to half cells, the increase in the CTM_{power} ratio of half-cell modules overcompensates the additional production costs. Specific costs (€/Wp) of half-cell modules are subsequently reduced for this module designs. We find an advantage of up to 1% for specific costs of half cell modules.

REFERENCES

[1] S. Guo, J. P. Singh, I. M. Peters, A. G. Aberle, and T. M. Walsh, "A quantitative analysis of photovoltaic modules using halved cells," *International Journal of Photoenergy*, vol. 2013, pp. 1–8, 2013.

[2] S. Zhang *et al.*, "335Watt world record P-type mono-crystalline module with 20.6 % efficiency PERC solar cells," in *2015 IEEE 42nd Photovoltaic Specialist Conference (PVSC): 14-19 June 2015, New Orleans, LA*, New Orleans, LA, 2015, pp. 1–6.

[3] A. J. Beinert, P. Romer, M. Heinrich, M. Mittag, and Neuhaus, Dirk Holger, Aktaa, Jarir, "Thermomechanical Evaluation of New PV Module Designs by FEM Simulations," in *Proceedings of the 36th European Photovoltaic Solar Energy Conference and Exhibition (EU PVSEC); Marseille, France*, 2019.

[4] ITRPV, "International Technology Roadmap for Photovoltaic (ITRPV): 10th edition, 2018 Results," 2019. Accessed on: Apr. 23 2019.

[5] M. Mittag *et al.*, "Cell-to-Module (CTM) analysis for photovoltaic modules with shingled solar cells," in *44th IEEE PV Specialist Conference PVSC*.

[6] M. Mittag and M. Ebert, "Systematic PV module optimization with the cell-to-module (CTM) analysis software," *Photovoltaics International*, no. 36, pp. 97–104, 2017.

[7] I. Hädrich, U. Eitner, M. Wiese, and H. Wirth, "Unified methodology for determining CTM ratios: Systematic prediction of module power," *Sol Energ Mat Sol C*, vol. 131, pp. 14–23, 2014.

[8] M. Mittag *et al.*, "Analysis of backsheet and rear cover reflection gains for bifacial solar cells," *33rd European PV Solar Energy Conference and Exhibition*, vol. 2017.

[9] M. Mittag *et al.*, "Electrical and thermal modeling of junction boxes," in *Proceedings of the 33rd European Photovoltaic Solar Energy Conference and Exhibition (EU PVSEC)*, Amsterdam, 2017, pp. 1501–1506.

[10] A. Pfreundt, M. Mittag, M. Heinrich, and U. Eitner, "Rapid Calculation of the Backsheet Coupling Gain Using Ray Groups," *32nd European Photovoltaic Solar Energy Conference and Exhibition (EUPVSEC)*, 2018.

[11] J. Shahid, M. Mittag, and M. Heinrich, "A Multidimensional Optimization Approach to Improve Modoule efficiency, power and costs," in *Proceedings of the 35th European Photovoltaic Solar Energy Conference and Exhibition (EU PVSEC); Brussels, Belgium*, 2018.

[12] M. Mittag, L. Vogt, C. Herzog, and D. H. Neuhaus, "Thermal Modelling of Photovoltaic Modules in Operation and Production," in *36th European Photovoltaic Solar Energy Conference and Exhibition (EUPVSEC) 2019*.

[13] F. Fertig *et al.*, "Economic feasibility of bifacial silicon solar cells," *Prog. Photovolt: Res. Appl.*, n/a-n/a, 2016.

[14] S. Nold *et al.*, "Cost Modelling of Silicon Solar Cell Production Innovation Along the PV Value Chain," in *Proceedings of the 27th European*

Photovoltaic Solar Energy Conference and Exhibition, Frankfurt, Germany, 2012.
[15] M. Mittag *et al.*, "Approach for a Holistic Optimization from Wafer to PV System," in *Proceedings of the 7th World Conference on Photovoltaic Energy Conversion*, Hawaii, 2018.
[16] D. C. Walter, B. Lim, and J. Schmidt, "Realistic efficiency potential of next-generation industrial Czochralski-grown silicon solar cells after deactivation of the boron-oxygen-related defect center," *Prog. Photovolt: Res. Appl.*, vol. 24, no. 7, pp. 920–928, 2016.
[17] S. Eiternick, K. Kaufmann, J. Schneider, and M. Turek, "Loss Analysis for Laser Separated Solar Cells," *Enrgy Proced*, vol. 55, pp. 326–330, 2014.
[18] A. Fell *et al.*, "Modeling Edge Recombination in Silicon Solar Cells," *IEEE J. Photovoltaics*, vol. 8, no. 2, pp. 428–434, 2018.
[19] N. Wöhrle *et al.*, "The SPEER solar cell – simulation study of shingled PERC technology based stripe cells," in *33rd EU PVSEC*, Amsterdam, The Netherlands, 2017.
[20] A. Fell, J. Schön, M. C. Schubert, and S. W. Glunz, "The concept of skins for silicon solar cell modeling," *Sol. Energy Mater. Sol. Cells*, vol. 173, pp. 128–133, 2017.
[21] S.-I. P.J. *et al.*, "Microsoft Word - 1CV1_40.docPerformance of Photovoltaic Modules with White Reflective Back Sheets," in *Proceedings of the 23rd European Photovoltaic Solar Energy Conference and Exhibition*, Valencia, Spain, 2008.
[22] S. Regondi, H. Hanifi, and J. Schneider, "Modeling and Simulation of the Influence of Interconnection Losses on Module Temperature in Moderate and Desert Regions," *IEEE J. Photovoltaics*, pp. 1–7, 2019.
[23] H. Hanifi, C. Pfau, M. Turek, and J. Schneider, "A practical optical and electrical model to estimate the power losses and quantification of different heat sources in silicon based PV modules," *Renewable Energy*, vol. 127, pp. 602–612, 2018.